Supporting Information

for

Tracking Source Variations of Inhalation Cancer Risks and Ozone Formation Potential in Hong Kong over Two Decades (2000–2020) Using Toxic Air Pollutant Monitoring Data

Yee Ka Wong[1], Wai Wai Chan[2], Dasa Gu[1], Jian Zhen Yu[1,2,3,*], Alexis K. H. Lau[1,2,4,*]

[1]Division of Environment and Sustainability, The Hong Kong University of Science and Technology, Clear Water Bay, Kowloon, Hong Kong 000000, China

[2]Institute for the Environment, The Hong Kong University of Science and Technology, Clear Water Bay, Kowloon, Hong Kong 000000, China

[3]Department of Chemistry, The Hong Kong University of Science and Technology, Clear Water Bay, Kowloon, Hong Kong 000000, China

[4]Department of Civil and Environmental Engineering, The Hong Kong University of Science and Technology, Clear Water Bay, Kowloon, Hong Kong 000000, China

*Corresponding author – Jian Zhen Yu; Division of Environment and Sustainability, Institute for the Environment, Department of Chemistry, The Hong Kong University of Science and Technology, Clear Water Bay, Kowloon, Hong Kong, China; Email: jian.yu@ust.hk

*Corresponding author – Alexis Kai Hon Lau; Division of Environment and Sustainability, Institute for the Environment, Department of Civil and Environmental Engineering, The Hong Kong University of Science and Technology, Clear Water Bay, Kowloon, Hong Kong, China; Email: alau@ust.hk

S1 Further details on PMF model inputs and source identification methods

Species that were measured above method detection limits (MDLs) in more than 75% of the time were included in the model. The input species uncertainties were represented by the square root of the squared sum of measurement uncertainty and half MDLs.[1] Concentrations below MDLs were replaced with half MDLs with uncertainties set to be 5/6 × MDL. The sample sizes for CW and TW are 484–496 for VOCs, 244 for carbonyls, 243–247 for PAHs, and 1087–1135 for PM_{10}.

For source identification, we determined the optimal factor number based on the statistical stability of the solution and interpretability of resolved source factors. The former was evaluated using the bootstrapping and displacement functions embedded in the PMF software. The results are provided in Table S4, showing all the PMF solutions are statistically robust for source analysis. Emission sources were identified through examination of the chemical profiles and temporal variation patterns of individual factors.

To distinguish between primary and secondary sources of carbonyls, collocated measurements of NO_x and O_3 (daily averaged from hourly data from reference monitors) were included in the model. The differentiation was aided by the use of nitric oxide and O_3 as a marker for primary and secondary formation, respectively. Table S5 tabulates the ratio of modeled vs. measured concentration for individual TAPs. Averaged across both sites and individual TAP groups, the models explained 91%, 78%, 78% and 97% of the observed concentrations of VOCs, carbonyls (with O_3 and NO_x), PAHs and PM_{10} species, respectively.

In the PMF analysis for VOCs, a source factor representing construction/renovation activities at or adjacent to the sampling location were resolved at both sites. Given these sources are not representative of the general air quality, they were excluded from subsequent risk and ozone impact calculations to avoid biased assessments. During the affected period, substantial enhancement in concentrations of certain carbonyls commonly found in solvents such as formaldehyde and benzaldehyde is noticed. However, the PMF model was not able to resolve a solution that includes this factor while being statistically robust (i.e., failed in the bootstrapping and displacement analyses) as the PMF for VOC did, plausibly due to insufficient sample size that prohibits the determination of a statistically robust solution. As a compromise, we down-weighted the carbonyls that were clearly affected by the construction/renovation in the model. Using this approach, while the model was unable to capture the high concentrations for the construction/renovation periods, it successfully apportioned concentrations that agree well with measurements outside the affected periods as shown in Figure S1. This also explains the lower ratio in modeled-to-measured concentrations for certain carbonyls in Table S5.

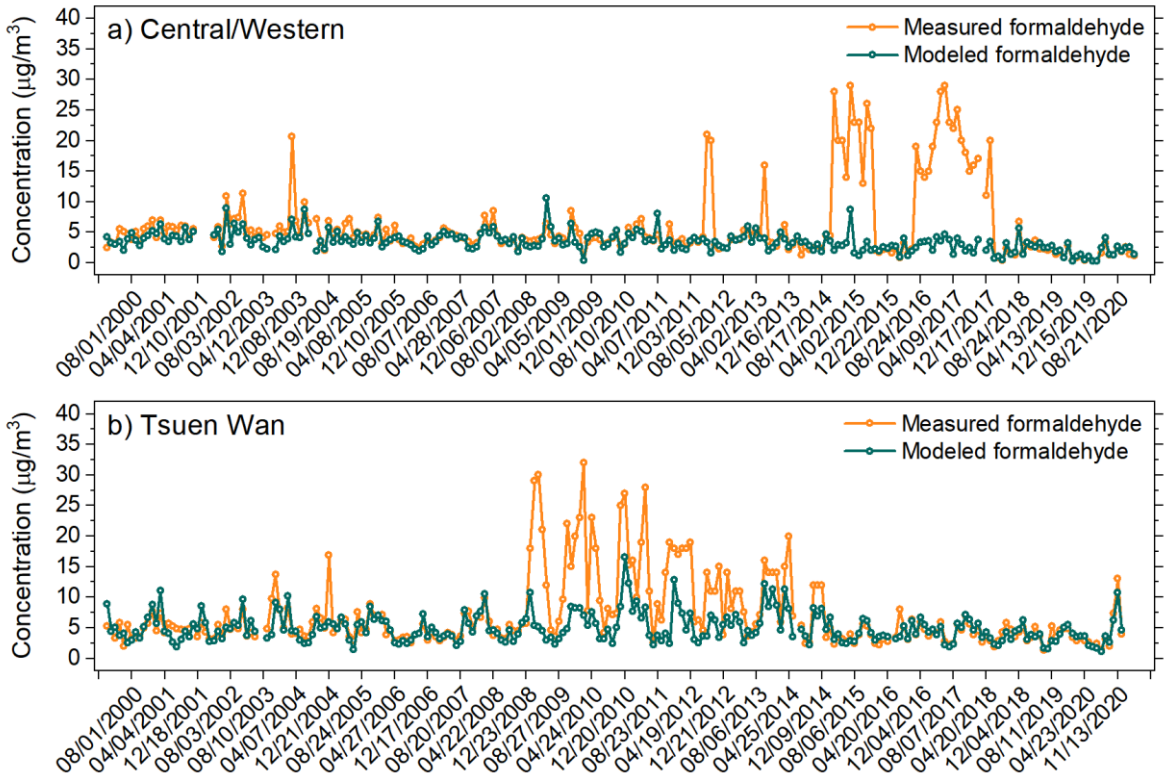

Figure S1. Time series of PMF-modeled versus measured concentrations of formaldehyde at (a) Central/Western and (b) Tsuen Wan sites. The discrepancy between modeled and measured concentration is attributed to the influence of local construction/renovation activities which are not captured in PMF modeling.

S2 Sources of TAPs identified by PMF analysis

The chemical profiles of the resolved factors for each TAP group at each site are presented in Figure S2. To aid source identification, we also examine the inter-annual and seasonal variations in the contributions of individual factors, which often show source-indicative characteristics. Figure S3 displays the inter-annual trends in source contributions for nine selected sources for VOCs, carbonyls and PAHs with the most significant ICR contributions, while those for the other sources are provided in Figures S4 and S5. For each source, the trends representing the mean contribution from warmer (April to September) and colder seasons (October to February) are shown, with the shaded bands representing the standard deviation. As a result of the synoptic-scale meteorological effect arising from the Asiatic monsoon, Hong Kong tends to receive relatively cleaner marine air masses from the south in warmer seasons but more polluted air masses from the northern inland regions in colder seasons.[2] Hence, the warm season trend reflects more the impact of local emissions while the cold season trend is more reflective of the impact of regional transport of pollutants emitted from the inland regions. Also shown in each plot are the Theil-Sen's slope values representing the rate of change in source contribution per year, and the significance level of Mann-Kendall trend test for statistical assessment of whether the change is monotonic over the study period.[3,4]

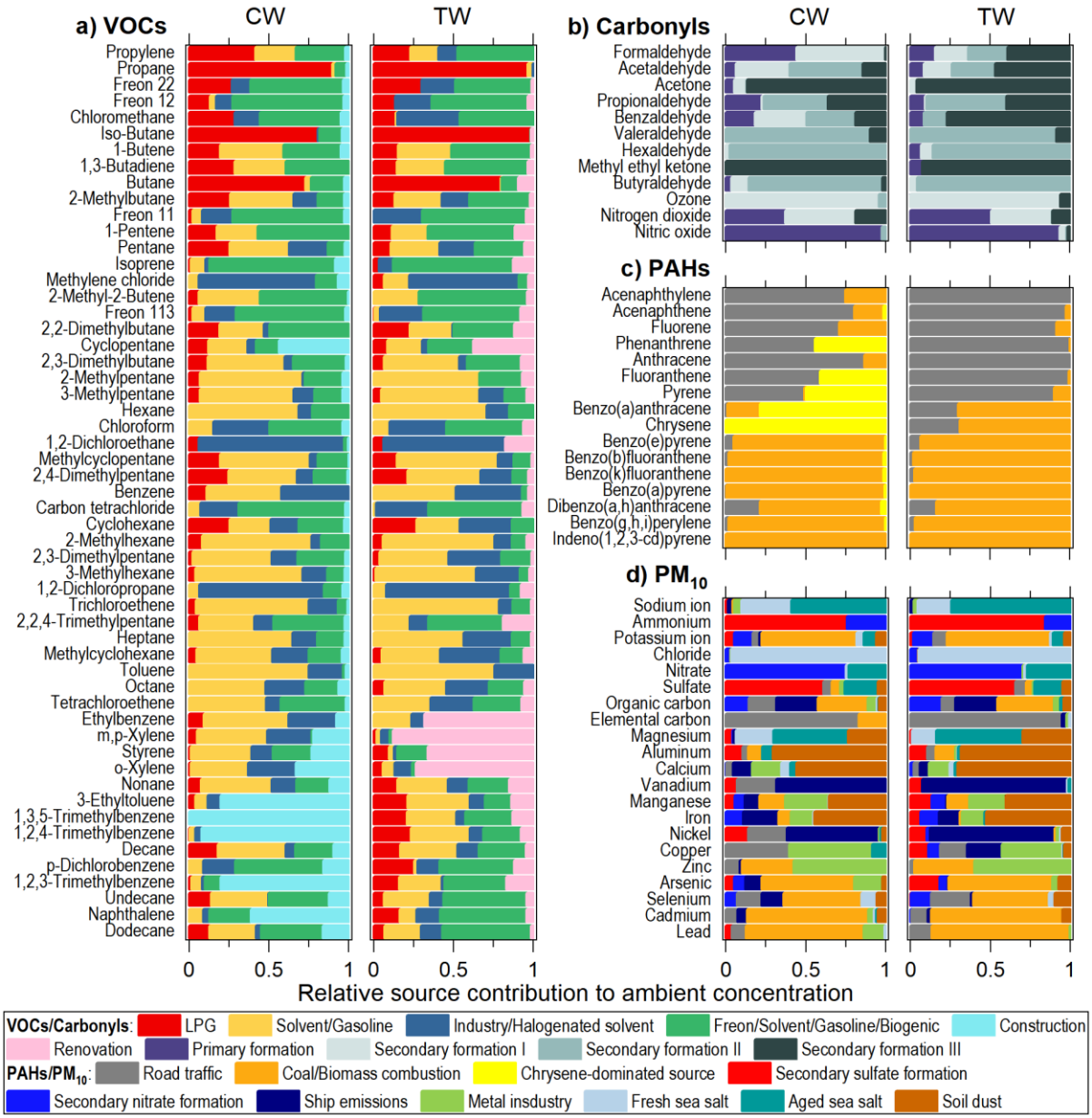

Figure S2. Source profiles derived from PMF analyses for (a) VOCs, (b) carbonyls, (c) PAHs, and (d) PM_{10}. For each TAP category, the left and right panels represent the results for CW and TW sites, respectively.

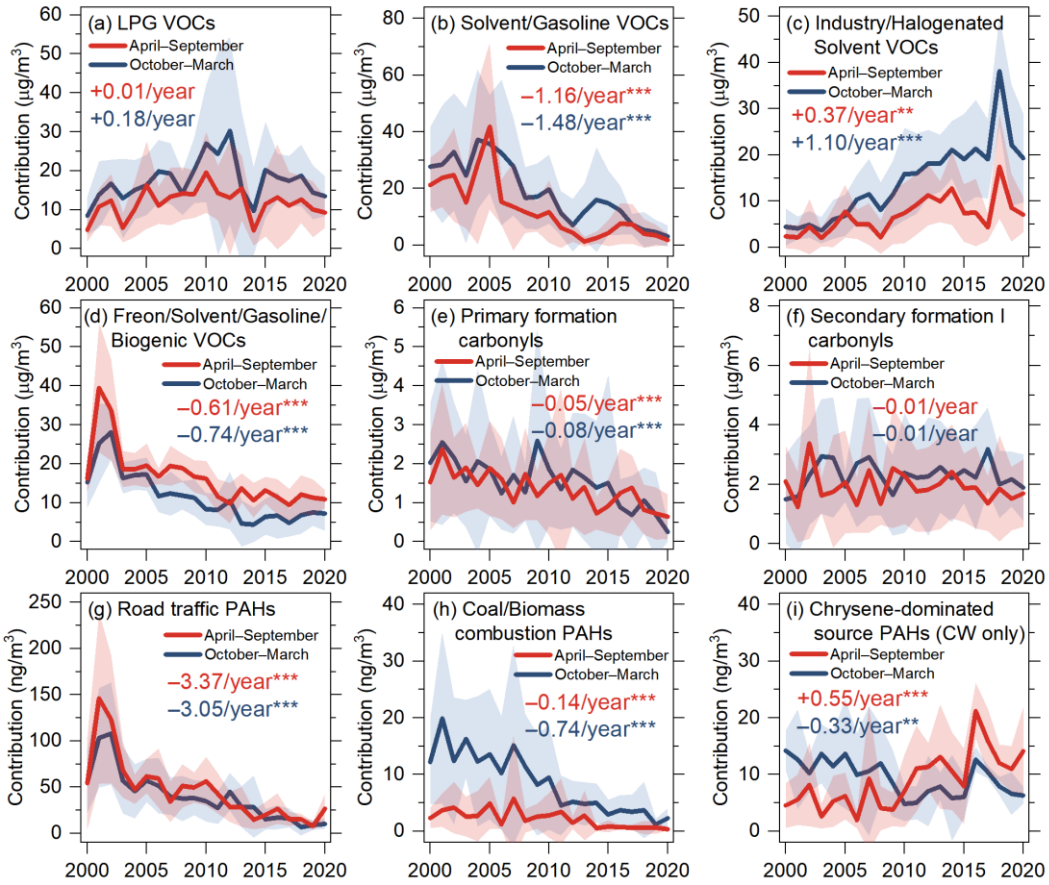

Figure S3. Inter-annual trends of source contributions to (a)–(d) VOCs, (e)–(f) carbonyls, and (g)–(i) PAHs averaged from CW and TW sites. The red and blue traces are the means derived from warmer months (i.e., April–September) and colder months (i.e., October–March) measurements, respectively, with the shaded bands representing ±1 standard deviation. Sen's slope and significance level of Mann-Kendall trend test (*: $p < 0.05$, **: $p < 0.01$, ***: $p < 0.001$) for warmer and colder months are displayed.

Sources of VOCs

Four common VOC source factors are resolved at the CW and TW sites, as shown in Figure S2a. The first factor is named LPG. It is marked by high loadings of propane, iso-butane, and butane, which are often regarded as emissions associated with the use of liquified petroleum gas (LPG) in motor vehicles, cooking and heating.[5] This factor exhibited an increasing trend up to 2012, which then reversed as shown in Figure S3a. This pattern coincides with the evolution of the contribution from LPG-fueled vehicles in Hong Kong over the last two decades, and the continuous drop after 2012 is attributed to a catalytic converter replacement program for LPG vehicles implemented by the local government.[6,7] Such a characteristic long-term variation indicates that local LPG-fueled vehicles are the main source in this factor. The higher contribution observed in colder seasons (Figure S3a) is attributed to multiple reasons, including reduced photochemical activity, increased influence from regional transport from inner continental region associated with prevailing northerlies, and meteorological conditions (e.g., less frequent precipitation and shallower boundary layer) more favorable to accumulation and elevation of pollutants.

The second factor is named solvent/gasoline, for the high abundance of branched and straight-chain alkanes and BTEX (benzene, toluene, ethylbenzene and xylenes) apportioned to this factor. Previous local studies have shown that these VOCs are primarily associated with emissions from solvent use and gasoline vehicles.[5,6,8] As noted from Figure S3b, this factor displayed a distinctive downward trend after 2005, consistent with the series of VOC control measures implemented by the local government in phases since mid-2000s. Example measures included controlling VOC content of architectural paints, printing inks, consumer products (e.g., air fresheners, hairsprays, lubricants, etc.), and other VOC-containing products (e.g., adhesives, sealants, vehicle refinish paints, etc.). Control measures were also implemented to recover gasoline vapor released during vehicle refueling at gas stations and to tighten emissions standards of motor vehicles in accordance with the European Union standards.[9] Owing to the similar reasons that apply to LPG, higher contribution in colder seasons is also noted for this source factor.

The third factor is named industry/halogenated solvent as supported by multiple lines of evidence. First, high loading of halogenated VOCs and BTEX is present in this factor (Figure S2a), which are typically the key chemical constituents found in industrial emissions and solvents.[5,10] Second, this factor shows a distinctly higher contribution in colder seasons when regional contribution enhances (Figure S3c), aligning with the much more widespread industrial and solvent-related sources located in mainland China that often impose an exacerbated impact on local air quality in colder seasons due to regional transport. Furthermore, this factor exhibited a continuous upward trend over the last two decades, coinciding with the persistent growth in industry- and solvent use-related VOCs in China over the same period as shown by the nationwide emission inventory.[11] In particular, the inventory showed that anthropogenic non-methane VOCs emissions in China associated with industry and solvent use combined had quadrupled from 4.9 Tg in 2000 to 19.6 Tg in 2017. Though not being necessarily directly correlated, the relative increase of VOC contribution of our industry/halogenated solvent factor in colder seasons is very close to the emission inventory estimates, increasing from 4.4 to 19.1 $\mu g/m^3$ in the corresponding period (Figure S3c).

The fourth factor is named freon/solvent/gasoline/biogenic. The chemical profile exhibits a mixture of 1) Freons suggestive of release of these ozone-depleting substances from chlorofluorocarbons-containing materials (e.g., cell foam and refrigeration system),[12] 2) chloroform and carbon tetrachloride suggestive of solvent use, 3) alkenes and higher molecular weight VOCs (naphthalene, undecane and dodecane) suggestive of gasoline evaporation, and 4) isoprene indicative of vegetative emissions. This factor has a higher contribution in warmer months (Figure S3d), which is consistent with a hypothesis that all these sources are increasingly active as temperature increases due to their evaporative nature.

The last factor resolved at CW and TW sites are named CW site construction and TW site renovation, respectively (Figure S2a). The identity of these sources is evident by the coincidence in time with these activities as documented by the monitoring department.[13] As shown in the temporal trends in Figure S4a, the remarkable enhancement in contribution at CW in 2015–2018 is attributed to construction works of a new subway station within 100 m of the sampling site in 2015 and at the community complex building housing the sampling equipment in 2016–2018. The enhanced contribution at TW occurred in 2009–2014 (Figure S4b) and is associated with renovation works within and near the community center where the sampling site is situated. The two sources also have differing composition, reflecting the different nature

of these man-made sources. For example, naphthalene is discernibly higher in CW construction than TW renovation, which can be explained by off-gassing of naphthalene from building materials.[14] As mentioned in Section 3.1 of the main text, these local sources will not be included in the assessments of health risks and O_3 formation in this study.

Sources of carbonyl compounds

Four carbonyl factors resembling a primary and three secondary formation sources are resolved at both locations (Figure S2b). The primary factor is signaled by a high loading of short-lived nitric oxide, which indicates primary emissions mainly traffic exhaust. The continuous declining trend and lack of seasonal variation in contribution support its nature (Figure S3e). The second to fourth factors are respectively named secondary formation I, II and III. Secondary formation I is heavily loaded with O_3 and nitrogen dioxide, which are associated with photochemical reactions. Secondary formation II and III differ in their abundance in the characteristic VOC oxidation products, with the former dominated by C_4 to C_6 aldehydes and the latter dominated by acetone and methyl ethyl ketone. The difference could be attributed to their differing photochemical formation and removal processes. All these secondary formation factors exhibit a higher contribution in colder months and no statistically significant inter-annual trend (Figures S3f and S4c&d).

Sources of PAHs

Two common PAH factors are identified at CW and TW sites (Figure S2c). The first factor has a high loading of 3–4-ring PAHs, with a lack of seasonality and noticeable declining trend in contribution (Figure S3g), indicating an association with local road traffic. The second factor is identified as coal/biomass combustion. This factor dominates the contributions of 4–6-ring PAHs. Previous studies based on receptor modeling and diagnostic ratio analyses have shown that these PAHs in Hong Kong and the GBA are mainly associated with coal combustion and biomass burning.[15,16] The considerably higher contribution in colder seasons combined with the continuous reduction shown in Figure S3h further supports the source identity, given these sources primarily spread over the inland GBA with continuous improvement in air quality over the years as a result of various air pollution control efforts.[17]

A third factor is resolved at the CW site, showing a markedly high loading of chrysene and benzo(a)anthracene, and some other 3–4-ring PAHs. The temporal variation of this factor differs from the others in that it exhibits a statistically significant ($p < 0.001$) upward trend during warmer seasons (Figure S3i). The benzo(a)anthracene / (benzo(a)anthracene + chrysene) and fluoranthene / (fluoranthene + pyrene) ratios of this factor are 0.18 and 0.47, respectively suggesting petrogenic emissions (e.g., release of uncombusted gasoline) and fossil fuel combustion.[18] While this factor is plausibly associated with traffic sources near the CW site, further study (possibly with higher time resolution measurement) is needed to identify its source origin(s). This factor is named chrysene-dominated source.

Sources of PM_{10}

Nine PM_{10} sources are resolved at both CW and TW sites. These identified sources are consistent with those established in previous source apportionment studies derived from the same PM_{10} speciation network data covering different periods, and hence they are not discussed in detail here.[17,19] Briefly, these factors are classified according to their characteristic markers, as illustrated in Figure S2d. These factors are secondary sulfate formation processes, secondary nitrate formation processes, road traffic, ship emissions, coal/biomass combustion, metal industry, fresh sea salt, aged sea salt, and soil dust. The seasonal inter-annual trends of these sources are provided in Figure S5.

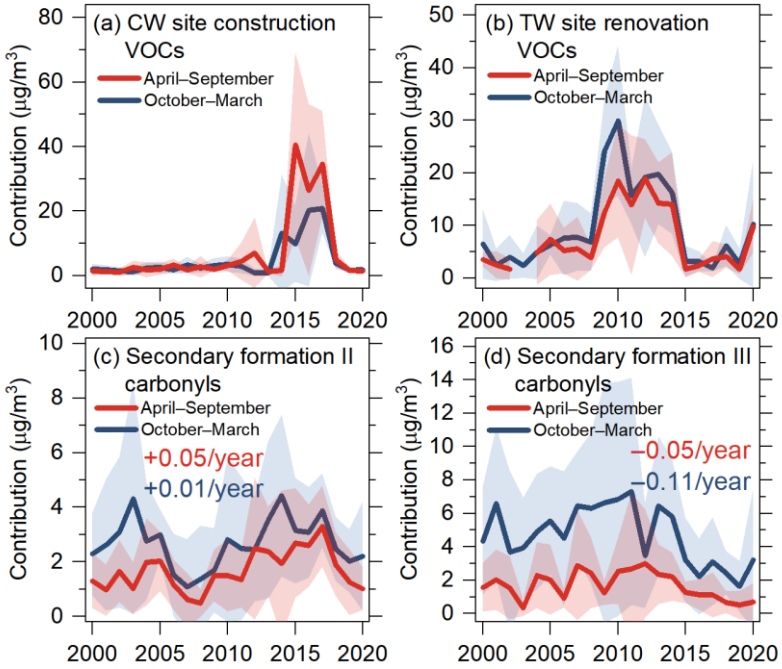

Figure S4. Inter-annual trends of source contributions to VOCs from (a) CW site construction and (b) TW site renovation, and to carbonyls from (c) secondary formation II and (d) secondary formation III. The red and blue traces are derived from warmer months (i.e., April–September) and colder months (i.e., October–March) measurements, respectively, with the shaded bands representing ±1 standard deviation. The trends in panels (c) and (d) are averaged from CW and TW sites, with Sen's slope and significance level of Mann-Kendall trend test (*: $p < 0.05$, **: $p < 0.01$, ***: $p < 0.001$) for warmer and colder months displayed.

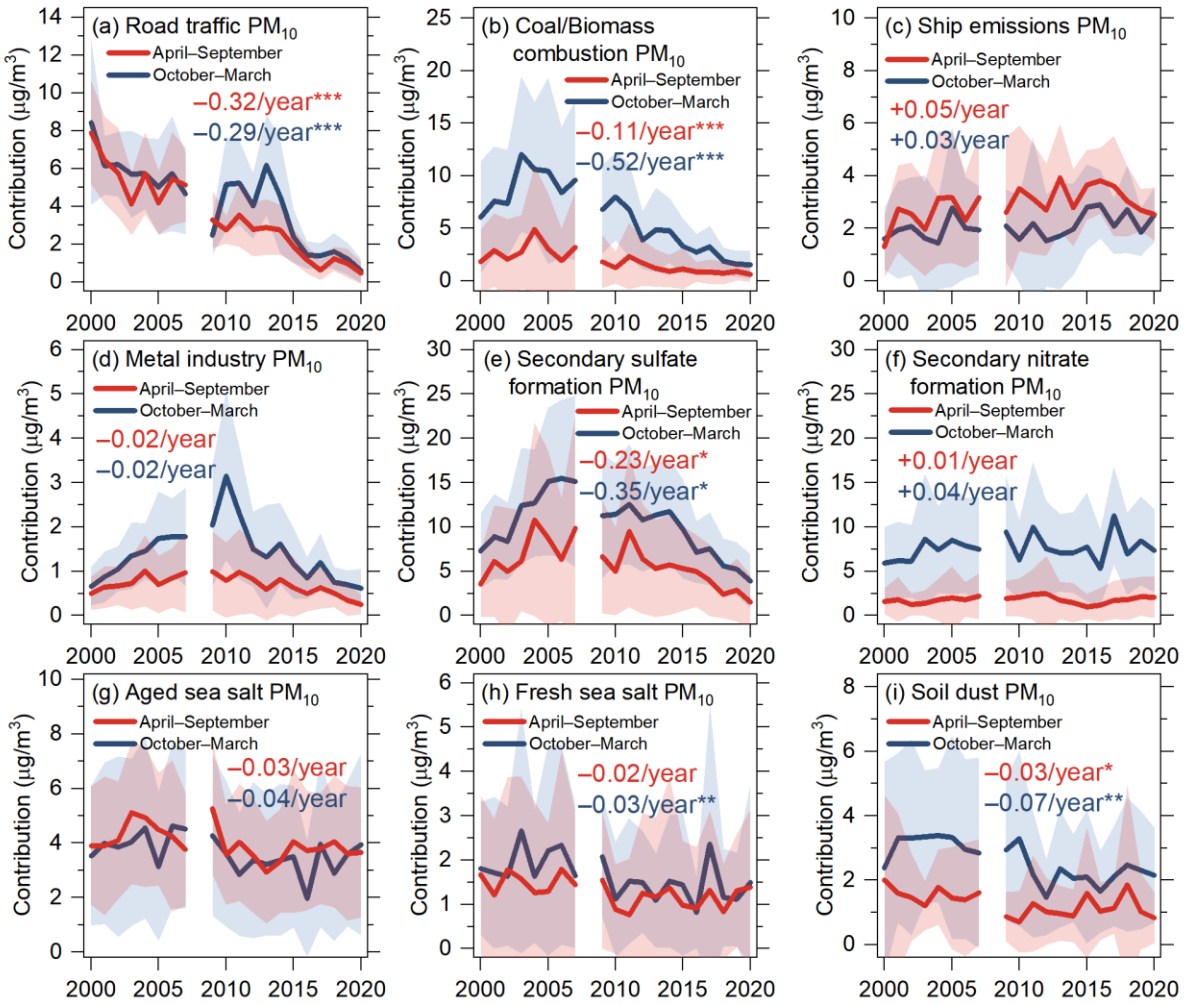

Figure S5. Inter-annual trends of source contributions to PM_{10} averaged from CW and TW sites. The red and blue traces are derived from warmer months (i.e., April–September) and colder months (i.e., October–March) measurements, respectively, with the shaded bands representing ±1 standard deviation. Sen's slope and significance level of Mann-Kendall trend test (*: $p < 0.05$, **: $p < 0.01$, ***: $p < 0.001$) for warmer and colder months are displayed.

Table S1. Toxic air pollutants examined in this study

VOCs (Sampling conducted twice a month)		
1,1,1-Trichloroethane	2-Methylhexane	Freon 12
1,1,2,2-Tetrachloroethane	2-Methylpentane	Freon 22
1,1,2-Trichloroethane	3,6-Dimethyloctane	Heptane
1,1-Dichloroethane	3-Chloropropene	Hexachlorobutadiene
1,1-Dichloroethene	3-Ethyltoluene	Hexane
1,2,3,5-Tetramethylbenzene	3-Methyl-1-Pentene	Hexylbenzene
1,2,3-Trimethylbenzene	3-Methylheptane	Indan
1,2,4,5-Tetramethylbenzene	3-Methylhexane	iso-Butane
1,2,4-Trichlorobenzene	3-Methylpentane	iso-Butylbenzene
1,2,4-Trimethylbenzene	4-Ethyltoluene	Isoprene
1,2,4-Trimethylcyclohexane	4-Methyl-1-Pentene	iso-Propylbenzene
1,2-Dibromoethane	4-Methylheptane	m,p-Xylene
1,2-Dichloroethane	Benzene	m-/p-Chlorotoluene
1,2-Dichloropropane	Benzyl chloride	m-Dichlorobenzene
1,2-Diethylbenzene	Bromodichloromethane	Methylcyclohexane
1,3,5-Trimethylbenzene	Bromoethane	Methylcyclopentane
1,3-Butadiene	Bromoform	Methylene chloride
1,3-Diethylbenzene	Bromomethane	Naphthalene
1,4-Dichlorobutane	Bromotrichloromethane	n-Butylbenzene
1,4-Diethylbenzene	Butane	Nonane
1-Butene	Carbon tetrachloride	n-Propylbenzene
1-Butyne	Chlorobenzene	o-Chlorotoluene
1-Decene	Chloroethane	Octane
1-Heptene	Chloroethene	o-Dichlorobenzene
1-Methylcyclohexene	Chloroform	o-Xylene
1-Methylcyclopentene	Chloromethane	p-Cymene
1-Nonene	cis-1,2-Dichloroethene	p-Dichlorobenzene
1-Octene	cis-1,2-Dimethylcyclohexane	Pentane
1-Pentene	cis-1,3-Dichloropropene	Propane
1-Propyne	cis-2-Butene	Propylene
2,2,3-Trimethylbutane	cis-2-Heptene	sec-Butylbenzene
2,2,4-Trimethylpentane	cis-2-Hexene	Styrene
2,2,5-Trimethylhexane	cis-2-Pentene	tert-Butylbenzene
2,2-Dimethylbutane	cis-3-Heptene	Tetrachloroethene
2,2-Dimethylhexane	cis-3-Methyl-2-Pentene	Toluene
2,2-Dimethylpropane	cis-4-Methyl-2-Pentene	trans-1,2-Dichloroethene
2,3,4-Trimethylpentane	Cyclohexane	trans-1,2-Dimethylcyclohexane
2,3-Dimethylbutane	Cyclohexene	trans-1,3-Dichloropropene
2,3-Dimethylpentane	Cyclopentane	trans-2-Butene
2,4-Dimethylhexane	Cyclopentene	trans-2-Heptene
2,4-Dimethylpentane	Decane	trans-2-Hexene
2,5-Dimethylhexane	Dibromochloromethane	trans-2-Pentene
2-Ethyl-1-Butene	Dibromomethane	trans-3-Heptene
2-Ethyltoluene	Dodecane	trans-3-Methyl-2-Pentene
2-Methyl-1-Butene	Ethylbenzene	trans-4-Methyl-2-Pentene
2-Methyl-2-Butene	Freon 11	Trichloroethene
2-Methylbutane	Freon 113	Undecane
2-Methylheptane	Freon 114	Xylenes
Carbonyls (Sampling conducted once a month)		
2,5-Dimethylbenzaldehyde	Crotonaldehyde	o-Tolualdehyde
Acetaldehyde	Formaldehyde	Propionaldehyde
Acetone	Hexaldehyde	p-Tolualdehyde
Acrolein	Isovaleraldehyde	Valeraldehyde
Benzaldehyde	Methyl ethyl ketone	
Butyraldehyde/IBA	m-Tolualdehyde	

Table S1. Continued

PAHs (Sampling conducted once a month)		
Acenaphthene	Benzo(e)pyrene	Fluorene
Acenaphthylene	Benzo(g,h,i)perylene	Indeno(1,2,3-cd)pyrene
Anthracene	Benzo(k)fluoranthene	Phenanthrene
Benzo(a)anthracene	Chrysene	Pyrene
Benzo(a)pyrene	Dibenzo(a,h)anthracene	
Benzo(b)fluoranthene	Fluoranthene	
Diesel PM and metal(loid)s (Sampling conducted once every six days)		
Diesel PM	Nickel	Selenium
Arsenic	Lead	Hexavalent chromium
Beryllium	Manganese	
Cadmium	Mercury	

Table S2. Unit risk estimates (URE) for individual toxic air pollutants and their average concentrations measured at Central/Western (CW) and Tsuen Wan (TW) sites in 2000–2004 and 2016–2020

Toxic air pollutants	URE, $(ug/m^3)^{-1}$	Average concentration in 2000-2004, ng/m^3		Average concentration in 2016-2020, ng/m^3	
		CW	TW	CW	TW
VOCs					
1,2-Dibromoethane	6.0E-04[a]	140.3*	138.2*	80.0*	80.0*
Benzene	2.9E-05[b]	1877.5	2610.6	1141.1	1514.7
Naphthalene	3.4E-05[a]	1511.7	1681.5	1283.0	1115.8
Carbon tetrachloride	4.2E-05[b]	930.6	982.8	698.5	701.2
1,2-Dichloroethane	2.6E-05[a]	192.8	202.1	741.9	786.8
1,3-Butadiene	1.7E-04[b]	199.7	306.3	51.0	76.9
p-Dichlorobenzene	1.1E-05[a]	599.5	487.6	840.6	446.5
1,2-Dichloropropane	1.0E-05[b]	173.0	172.3	474.8	484.9
1,1,2,2-Tetrachloroethane	5.8E-05[b]	167.4	181.7	70.0*	70.0*
Methylene chloride	1.0E-06[b]	2849.7	2915.5	4981.2	3505.4
Tetrachloroethene	6.1E-06[b]	2056.1	879.8	542.4	500.2
Ethylbenzene	2.5E-06[a]	1446.4	1811.3	896.2	1141.5
Chloroethene	7.8E-05[b]	73.4	73.8	37.9*	35.9*
Bromodichloromethane	3.7E-05[b]	347.3	331.9	70.0*	70.0*
Benzyl chloride	4.9E-05[a]	82.7*	92.9*	50.0*	51.4*
Hexachlorobutadiene	2.2E-05[a]	350.6	399.4	110.0*	110.0*
Chloroform	5.3E-06[b]	648.8	659.1	562.8	436.7
Trichloroethene	4.1E-06[a]	786.1	1561.6	212.7	288.8
1,1,2-Trichloroethane	1.6E-05[a]	92.3*	92.1*	65.3*	64.1*
3-Chloropropene	6.0E-06[a]	57.3	73.8	30.0*	31.2*
Bromoform	1.1E-06[a]	227.3	236.5	115.9*	120.3*
1,1-Dichloroethane	1.6E-06[a]	98.5	105.8	41.7*	40.6*
Carbonyls					
Formaldehyde	1.3E-05[a]	5674.5	5462.1	1742.9	3959.0
Acetaldehyde	2.7E-06[b]	2287.2	2386.6	1140.6	1822.1
PAHs					
Dibenzo(a,h)anthracene	4.4E-01[c]	0.0	0.1	0.0	0.0
Benzo(a)pyrene	8.7E-02[c]	0.3	0.4	0.0	0.1
Chrysene	8.7E-03[c]	0.5	0.7	0.6	0.3
Indeno(1,2,3-cd)pyrene	2.0E-02[c]	0.4	0.6	0.1	0.1
Benzo(b)fluoranthene	1.2E-02[c]	0.5	0.7	0.1	0.1
Fluoranthene	8.7E-04[c]	4.1	9.1	2.0	1.2
Benzo(k)fluoranthene	8.7E-03[c]	0.2	0.3	0.0	0.1
Benzo(a)anthracene	1.3E-03[c]	0.3	0.4	0.2	0.1
Diesel PM / Metal(loid)s					
Diesel PM	3.0E-04[b]	3744.8	5358.9	719.4	885.8
Hexavalent chromium	1.5E-01[b]	0.2	0.2	0.1*	0.1*
Arsenic	4.3E-03[a]	4.2	5.2	2.5	2.5
Cadmium	4.2E-03[b]	1.6	2.0	0.5	0.5
Nickel	3.8E-04[c]	5.2	6.0	3.9*	4.4*
Lead	1.2E-05[b]	56.3	71.5	12.473	13.4
Beryllium	2.4E-03[a]	0.1*	0.1*	0.1*	0.1*

[a]From the Office of Air Quality Planning and Standards of the U.S. EPA; [b]From the Office of Environmental Health Hazard Assessment of the California Environmental Protection Agency; [c]From the Guidelines for Air Quality of the World Health Organization.

Note: Concentrations labeled with an asterisk denotes the average value is below method detection limit. Half detection limit was used to calculate the average concentration for below detection limit data. These species were mostly not included in the PMF analyses of this study.

Table S3. Human carcinogenicity classification by the International Agency for Research on Cancer (IARC) for TAPs considered in the PMF source apportionment analyses in this study

Toxic air pollutants	IARC group	Definition
Formaldehyde	1	Carcinogenic to humans
Benzene	1	Carcinogenic to humans
Carbon tetrachloride	2B	Possibly carcinogenic to humans
1,2-Dichloroethane	2B	Possibly carcinogenic to humans
Naphthalene	2B	Possibly carcinogenic to humans
1,3-Butadiene	1	Carcinogenic to humans
Acetaldehyde	2B	Possibly carcinogenic to humans
1,2-Dichloropropane	1	Carcinogenic to humans
p-Dichlorobenzene	2B	Possibly carcinogenic to humans
Methylene chloride	2A	Probably carcinogenic to humans
Tetrachloroethene	2A	Probably carcinogenic to humans
Chloroform	2B	Possibly carcinogenic to humans
Ethylbenzene	2B	Possibly carcinogenic to humans
Trichloroethene	1	Carcinogenic to humans
Arsenic	1	Carcinogenic to humans
Chrysene	2B	Possibly carcinogenic to humans
Benzo(a)pyrene	1	Carcinogenic to humans
Dibenzo(a,h)anthracene	2A	Probably carcinogenic to humans
Nickel	1	Carcinogenic to humans
Cadmium	1	Carcinogenic to humans
Fluoranthene	3	Not classifiable as to its carcinogenicity to humans
Indeno(1,2,3-cd)pyrene	2B	Possibly carcinogenic to humans
Benzo(b)fluoranthene	2B	Possibly carcinogenic to humans
Benzo(k)fluoranthene	2B	Possibly carcinogenic to humans
Benzo(a)anthracene	2B	Possibly carcinogenic to humans
Lead	2A	Probably carcinogenic to humans

Table S4. Summary of PMF bootstrap and displacement results for VOCs, carbonyls, PAHs and PM_{10} in this study

			VOCs at CW			
DISP Diagnostics:	Error Code:	0	Largest Decrease in Q:	-5.254	%dQ:	-0.00199
	Swaps by Factor:	0	0	0	0	0
BS Mapping:	Factor 1	Factor 2	Factor 3	Factor 4	Factor 5	Unmapped
Boot Factor 1	79	0	0	4	17	0
Boot Factor 2	3	80	3	4	10	0
Boot Factor 3	3	0	96	1	0	0
Boot Factor 4	0	0	0	100	0	0
Boot Factor 5	0	0	0	0	100	0
			VOCs at TW			
DISP Diagnostics:	Error Code:	0	Largest Decrease in Q:	0	%dQ:	0
	Swaps by Factor:	0	0	0	0	0
BS Mapping:	Factor 1	Factor 2	Factor 3	Factor 4	Factor 5	Unmapped
Boot Factor 1	81	0	11	7	1	0
Boot Factor 2	0	100	0	0	0	0
Boot Factor 3	0	0	100	0	0	0
Boot Factor 4	1	0	5	87	7	0
Boot Factor 5	0	0	0	0	100	0
			Carbonyls at CW			
DISP Diagnostics:	Error Code:	0	Largest Decrease in Q:	0	%dQ:	0
	Swaps by Factor:	0	0	0	0	
BS Mapping:	Factor 1	Factor 2	Factor 3	Factor 4	Unmapped	
Boot Factor 1	100	0	0	0	0	
Boot Factor 2	0	100	0	0	0	
Boot Factor 3	0	0	100	0	0	
Boot Factor 4	7	13	0	80	0	
			Carbonyls at TW			
DISP Diagnostics:	Error Code:	0	Largest Decrease in Q:	-0.015	%dQ:	-6.6E-05
	Swaps by Factor:	0	0	0	0	
BS Mapping:	Factor 1	Factor 2	Factor 3	Factor 4	Unmapped	
Boot Factor 1	100	0	0	0	0	
Boot Factor 2	0	99	0	1	0	
Boot Factor 3	0	0	100	0	0	
Boot Factor 4	0	10	0	90	0	

Table S4. Continued

				PAHs at CW						
DISP Diagnostics:	Error Code:	0	Largest Decrease in Q:	0	%dQ:	0				
	Swaps by Factor:	0	0	0						
BS Mapping:	Factor 1	Factor 2	Factor 3	Unmapped						
Boot Factor 1	100	0	0	0						
Boot Factor 2	6	90	4	0						
Boot Factor 3	0	0	100	0						
				PAHs at TW						
DISP Diagnostics:	Error Code:	0	Largest Decrease in Q:	0	%dQ:	0				
	Swaps by Factor:	0	0							
BS Mapping:	Factor 1	Factor 2	Unmapped							
Boot Factor 1	100	0	0							
Boot Factor 2	0	100	0							
				PM_{10} at CW						
DISP Diagnostics:	Error Code:	0	Largest Decrease in Q:	-0.008	%dQ:	-8.1E-05				
	Swaps by Factor:	0	0	0	0	0	0	0	0	0
BS Mapping:	Factor 1	Factor 2	Factor 3	Factor 4	Factor 5	Factor 6	Factor 7	Factor 8	Factor 9	Unmapped
Boot Factor 1	100	0	0	0	0	0	0	0	0	0
Boot Factor 2	0	89	0	0	8	3	0	0	0	0
Boot Factor 3	0	0	100	0	0	0	0	0	0	0
Boot Factor 4	0	0	0	100	0	0	0	0	0	0
Boot Factor 5	0	0	0	0	100	0	0	0	0	0
Boot Factor 6	0	0	0	0	0	100	0	0	0	0
Boot Factor 7	0	0	0	0	0	1	99	0	0	0
Boot Factor 8	0	0	0	0	0	0	0	100	0	0
Boot Factor 9	0	0	0	0	0	0	0	0	100	0
				PM_{10} at TW						
DISP Diagnostics:	Error Code:	0	Largest Decrease in Q:	0	%dQ:	0				
	Swaps by Factor:	0	0	0	0	0	0	0	0	0
BS Mapping:	Factor 1	Factor 2	Factor 3	Factor 4	Factor 5	Factor 6	Factor 7	Factor 8	Factor 9	Unmapped
Boot Factor 1	100	0	0	0	0	0	0	0	0	0
Boot Factor 2	0	98	0	0	0	0	0	0	2	0
Boot Factor 3	0	0	100	0	0	0	0	0	0	0
Boot Factor 4	0	0	0	100	0	0	0	0	0	0
Boot Factor 5	0	0	0	0	100	0	0	0	0	0
Boot Factor 6	0	0	0	0	0	100	0	0	0	0
Boot Factor 7	0	0	0	0	0	0	100	0	0	0
Boot Factor 8	0	0	0	0	0	0	0	100	0	0
Boot Factor 9	0	0	0	0	0	0	0	0	100	0

Table S5. Ratio of PMF-modeled versus measured species concentrations at CW and TW sites

Ratio of PMF-modeled vs. measured concentration					
VOCs	CW	TW	*Carbonyls*	CW	TW
1,2,3-Trimethylbenzene	1.02	1.02	Acetaldehyde	0.94	0.91
1,2,4-Trimethylbenzene	0.92	0.88	Acetone	0.79	0.61
1,2-Dichloroethane	0.96	0.91	Benzaldehyde	0.81	0.38
1,2-Dichloropropane	0.98	0.97	Butyraldehyde/IBA	0.80	0.87
1,3,5-Trimethylbenzene	0.92	1.01	Formaldehyde	0.57	0.70
1,3-Butadiene	1.01	0.99	Hexaldehyde	0.82	0.85
1-Butene	0.91	0.89	Methyl ethyl ketone	0.73	0.32
1-Pentene	1.00	1.01	Propionaldehyde	0.85	0.84
2,2,4-Trimethylpentane	0.94	0.82	Valeraldehyde	0.77	0.65
2,2-Dimethylbutane	1.06	1.03	Ozone	0.86	0.95
2,3-Dimethylbutane	1.01	0.99	Nitrogen dioxide	0.88	0.95
2,3-Dimethylpentane	0.96	0.98	Nitric oxide	0.94	0.92
2,4-Dimethylpentane	1.01	1.01			
2-Methyl-2-Butene	1.03	1.01	*PAHs*	CW	TW
2-Methylbutane	0.91	0.89	Acenaphthene	0.78	0.74
2-Methylhexane	0.97	0.97	Acenaphthylene	0.53	0.58
2-Methylpentane	0.89	0.87	Anthracene	0.75	0.54
3-Ethyltoluene	0.98	0.94	Benzo(a)anthracene	0.60	0.53
3-Methylhexane	0.93	0.92	Benzo(a)pyrene	0.86	0.82
3-Methylpentane	0.92	0.91	Benzo(b)fluoranthene	0.97	0.93
Benzene	0.81	0.73	Benzo(e)pyrene	0.84	0.76
Butane	0.92	0.93	Benzo(g,h,i)perylene	0.93	0.94
Carbon tetrachloride	0.97	0.97	Benzo(k)fluoranthene	0.96	0.90
Chloroform	0.92	0.97	Chrysene	0.76	0.63
Chloromethane	0.93	0.92	Dibenzo(a,h)anthracene	0.74	0.66
Cyclohexane	0.74	0.76	Fluoranthene	0.85	0.75
Cyclopentane	0.91	0.93	Fluorene	0.81	0.70
Decane	0.92	0.85	Indeno(1,2,3-cd)pyrene	0.90	0.81
Dodecane	0.90	0.92	Phenanthrene	0.85	0.77
Ethylbenzene	0.86	0.90	Pyrene	0.92	0.91
Freon 11	0.97	0.95			
Freon 113	0.98	0.97	PM_{10}	CW	TW
Freon 12	0.96	0.94	Sodium ion	0.99	0.99
Freon 22	0.82	0.72	Ammonium	0.99	0.99
Heptane	0.89	0.87	Potassium ion	0.97	0.98
Hexane	0.90	0.92	Chloride	1.00	1.00
iso-Butane	0.95	0.92	Nitrate	0.99	0.97
Isoprene	0.69	0.78	Sulfate	1.00	0.99
m,p-Xylene	0.86	0.98	Organic carbon	0.95	0.95
Methylcyclohexane	0.90	0.86	Elemental carbon	0.97	0.99
Methylcyclopentane	0.98	0.98	Magnesium	0.97	0.97
Methylene chloride	0.69	0.66	Aluminum	0.93	0.91
Naphthalene	0.78	0.74	Calcium	0.97	0.97
Nonane	0.90	0.83	Vanadium	1.05	1.02
Octane	1.02	0.97	Manganese	0.99	0.99
o-Xylene	0.91	0.98	Iron	0.98	0.98
p-Dichlorobenzene	0.89	0.93	Nickel	1.07	1.07
Pentane	0.91	0.91	Copper	0.92	0.87
Propane	0.92	0.90	Zinc	0.94	0.95
Propylene	0.87	0.87	Arsenic	0.91	0.92
Styrene	0.80	0.18	Selenium	0.91	0.92
Tetrachloroethene	0.83	0.92	Cadmium	0.95	0.93
Toluene	0.91	0.91	Lead	0.95	0.96
Trichloroethene	0.88	0.89			
Undecane	0.94	0.93			

Table S6. Summary of Sen's slope values for source contributions to VOCs and carbonyls by mass in μg/m^3/year, OFP in μg-O_3/m^3/year and ICRs in cancer cases per million/year from 2000 to 2020 (percentage in parentheses is the slope normalized by 2000 level) and significance level of the Mann-Kendall trend test

		LPG	Solvent/ Gasoline	Industry/ Halogenated Solvent	Freon/Solvent/ Gasoline/ Biogenic	Primary formation	Secondary formation I to III
Mass	Sen's slope	+0.07 (+1.0%)	–1.34 (–5.5%)	+0.73 (+21.9%)	–0.69 (–4.4%)	–0.07 (–3.8%)	–0.05 (–0.8%)
	p-value	0.526	<0.001	<0.001	<0.001	<0.001	0.415
OFP	Sen's slope	+0.06 (+1.1%)	–2.42 (–5.5%)	+0.73 (+21.9%)	–0.63 (–4.1%)	–0.39 (–3.8%)	
	p-value	0.566	<0.001	<0.001	<0.001	<0.001	
ICRs	Sen's slope	+0.02 (+0.3%)	–3.31 (–5.5%)	+3.49 (+21.9%)	–2.55 (–4.4%)	–0.71 (–3.8%)	–0.30 (–0.7%)
	p-value	0.651	<0.001	<0.001	<0.001	<0.001	0.349

References

(1) Norris, G.; Duvall, R.; Brown, S.; Bai, S. Positive Matrix Factorization (PMF) 5.0 Fundamentals and User Guide. **2014**.

(2) Louie, P. K. K.; Watson, J. G.; Chow, J. C.; Chen, A.; Sin, D. W. M.; Lau, A. K. H. Seasonal Characteristics and Regional Transport of PM in Hong Kong. *Atmos. Environ.* **2005**, S1352231004011021. https://doi.org/10.1016/j.atmosenv.2004.11.017.

(3) Gilbert, R. O. *Statistical Methods for Environmental Pollution Monitoring*; Van Nostrand Reinhold Co: New York, 1987.

(4) Sen, P. K. Estimates of the Regression Coefficient Based on Kendall's Tau. *J. Am. Stat. Assoc.* **1968**, *63* (324), 1379–1389. https://doi.org/10.1080/01621459.1968.10480934.

(5) Lau, A. K. H.; Yuan, Z.; Yu, J. Z.; Louie, P. K. K. Source Apportionment of Ambient Volatile Organic Compounds in Hong Kong. *Sci. Total Environ.* **2010**, *408* (19), 4138–4149. https://doi.org/10.1016/j.scitotenv.2010.05.025.

(6) Lyu, X. P.; Zeng, L. W.; Guo, H.; Simpson, I. J.; Ling, Z. H.; Wang, Y.; Murray, F.; Louie, P. K. K.; Saunders, S. M.; Lam, S. H. M.; Blake, D. R. Evaluation of the Effectiveness of Air Pollution Control Measures in Hong Kong. *Environ. Pollut.* **2017**, *220*, 87–94. https://doi.org/10.1016/j.envpol.2016.09.025.

(7) Yao, D.; Lyu, X.; Murray, F.; Morawska, L.; Yu, W.; Wang, J.; Guo, H. Continuous Effectiveness of Replacing Catalytic Converters on Liquified Petroleum Gas-Fueled Vehicles in Hong Kong. *Sci. Total Environ.* **2019**, *648*, 830–838. https://doi.org/10.1016/j.scitotenv.2018.08.191.

(8) Ho, K. F.; Ho, S. S. H.; Lee, S. C.; Louie, P. K. K.; Cao, J.; Deng, W. Volatile Organic Compounds in Roadside Environment of Hong Kong. *Aerosol Air Qual. Res.* **2013**, *13* (4), 1331–1347. https://doi.org/10.4209/aaqr.2012.10.0278.

(9) HKEPD. *An Overview on Air Quality and Air Pollution Control in Hong Kong*. https://www.epd.gov.hk/epd/english/environmentinhk/air/air_maincontent.html (accessed 2023-12-11).

(10) Lyu, X.; Guo, H.; Wang, Y.; Zhang, F.; Nie, K.; Dang, J.; Liang, Z.; Dong, S.; Zeren, Y.; Zhou, B.; Gao, W.; Zhao, S.; Zhang, G. Hazardous Volatile Organic Compounds in Ambient Air of China. *Chemosphere* **2020**, *246*, 125731. https://doi.org/10.1016/j.chemosphere.2019.125731.

(11) Li, M.; Zhang, Q.; Zheng, B.; Tong, D.; Lei, Y.; Liu, F.; Hong, C.; Kang, S.; Yan, L.; Zhang, Y.; Bo, Y.; Su, H.; Cheng, Y.; He, K. Persistent Growth of Anthropogenic Non-Methane Volatile Organic Compound (NMVOC) Emissions in China during 1990–2017: Drivers, Speciation and Ozone Formation Potential. *Atmospheric Chem. Phys.* **2019**, *19* (13), 8897–8913. https://doi.org/10.5194/acp-19-8897-2019.

(12) Lickley, M.; Solomon, S.; Fletcher, S.; Velders, G. J. M.; Daniel, J.; Rigby, M.; Montzka, S. A.; Kuijpers, L. J. M.; Stone, K. Quantifying Contributions of Chlorofluorocarbon Banks to Emissions and Impacts on the Ozone Layer and Climate. *Nat. Commun.* **2020**, *11* (1), 1380. https://doi.org/10.1038/s41467-020-15162-7.

(13) HKEPD. *EPD - Air Quality Reports*. https://www.aqhi.gov.hk/en/download/air-quality-reports.html (accessed 2023-12-11).

(14) Jia, C.; Batterman, S. A Critical Review of Naphthalene Sources and Exposures Relevant to Indoor and Outdoor Air. *Int. J. Environ. Res. Public. Health* **2010**, *7* (7), 2903–2939. https://doi.org/10.3390/ijerph7072903.

(15) Liao, K.; Yu, J. Z. Abundance and Sources of Benzo[a]Pyrene and Other PAHs in Ambient Air in Hong Kong: A Review of 20-Year Measurements (1997–2016). *Chemosphere* **2020**, *259*, 127518. https://doi.org/10.1016/j.chemosphere.2020.127518.

(16) Wang, Q.; Feng, Y.; Huang, X. H. H.; Griffith, S. M.; Zhang, T.; Zhang, Q.; Wu, D.; Yu, J. Z. Nonpolar Organic Compounds as $PM_{2.5}$ Source Tracers: Investigation of Their Sources and Degradation in the Pearl River Delta, China. *J. Geophys. Res. Atmospheres* **2016**, *121* (19), 11,862-11,879. https://doi.org/10.1002/2016JD025315.

(17) Zhang, X.; Yuan, Z.; Li, W.; Lau, A. K. H.; Yu, J. Z.; Fung, J. C. H.; Zheng, J.; Yu, A. L. C. Eighteen-Year Trends of Local and Non-Local Impacts to Ambient PM_{10} in Hong Kong Based on Chemical Speciation and Source Apportionment. *Atmospheric Res.* **2018**, *214*, 1–9. https://doi.org/10.1016/j.atmosres.2018.07.004.

(18) Tobiszewski, M.; Namieśnik, J. PAH Diagnostic Ratios for the Identification of Pollution Emission Sources. *Environ. Pollut.* **2012**, *162*, 110–119. https://doi.org/10.1016/j.envpol.2011.10.025.

(19) Yuan, Z.; Yadav, V.; Turner, J. R.; Louie, P. K. K.; Lau, A. K. H. Long-Term Trends of Ambient Particulate Matter Emission Source Contributions and the Accountability of Control Strategies in Hong Kong over 1998–2008. *Atmos. Environ.* **2013**, *76*, 21–31. https://doi.org/10.1016/j.atmosenv.2012.09.026.